Analyses of Turbulence Parameters in the Near-Surface Layer at Qamdo of the Southeastern Tibetan Plateau

BIAN Lingen*[1] (卞林根), XU Xiangde[1] (徐祥德), LU Longhua[1] (陆龙骅), GAO Zhiqiu[1] (高志球), ZHOU Mingyu[2] (周明煜), and LIU Huizhi[3] (刘辉志)

[1] *Chinese Academy of Meteorological Sciences, Beijing* 100081

[2] *National Marine Environment Forecast Center, Beijing* 100081

[3] *Institute of Atmospheric Physics, Chinese Academy of Sciences, Beijing* 100029

(Received March 25, 2002; revised December 6, 2002)

ABSTRACT

The characteristics of the turbulence spectrum, turbulence variance, and turbulence flux at Qamdo over the Southeastern Tibetan Plateau measured during the TIPEX experiment from 18 May to 30 June 1998 are analyzed by the eddy correlation method. During periods of intense convection, most of the spectra of the 3D winds, temperature, and humidity follow a power law with a slope of -2/3. The normalized variances of the 3D winds in relation to z/L satisfy the similarity law but the normalized variances of temperature and humidity are related to z/L by a -1/3 power law only in unstable conditions. In near-neutral stratification, σ_u/u_* and σ_v/u_* at Qamdo and Gerze are nearly constant in rugged terrain and σ_w/u_* at Qamdo and Gerze is similar to the value found in plains, which indicates that the, effects of landform on vertical turbulence is not significant over the southeast and western Tibetan Plateau. During the dry period, the sensible heat dominates, comprising 81% of the heat intensity, with the other 19% being latent heat; during the wet period on the other hand, the latent heat accounts for about 64% of the available energy and the sensible heat only around 36%. The maximum intensity of the heating of air occurs in the middle of the Plateau during the summertime.

Key words: Tibetan Plateau, eddy correlation, turbulence variances, heat source

1. Introduction

Atmospheric dynamic and thermal effects over the Tibetan Plateau are dominated by surface-atmosphere interactions. The First Plateau Meteorological Experiment (QXPMEX) in 1979, substantially advanced our understanding of the radiation balance of the Plateau (Zhang et al., 1988). Unfortunately, however, its limited facilities available for sounding made it difficult to intensively observe and explore the structure of the Plateau's boundary layer and its turbulen transfer, particularly in the western and southeastern Plateau. As a result, the eddy correlation method was never used there. The second Tibetan Plateau Meteorological Experiment (TIPEX) was conceived to remedy this deficiency by focusing on measuring directional processes of turbulence transfer. TIPEX established sites for measuring the planetary boundary layer (PBL) structure at Gerze, Damxung, and Qamdo in the western, middle, and southeastern regions of the Plateau, respectively (Zhou et al., 2000). Advanced instrumentation was used to systematically measure 3D winds, temperature, and water vapor, along with the components of the radiation balance and profiles of soil temperature. Bian et al. (2001) and Li et al. (1999) reported the detailed measurements and analysis of the turbulence in the near-surface layer over the southeastern and the western Tibetan Plateau. This paper presents the characteristics of the turbulence spectrum and variances of 3D winds, temperature, and specific humidity, and it compares the heating intensity from the middle and western parts of the Plateau by the eddy correlation method. Both of these allow an understanding of the turbulence structure and boundary layer parameterization of the Plateau.

*E-mail: Bian Lingen blg@cams.cma.gov.cn

2. Turbulence spectrum

The spectra of atmospheric turbulence can reveal laws of motion and test data quality. Although spectral structures over a variety of underlying surfaces have been studied both by theory and experiment (Zhou et al., 1991; Panofsky et al., 1982), observations of the turbulence structure over the Tibetan Plateau have not yet been published.

We generated the turbulence spectrum of each variable in all of the 16384 samples by using fast Fourier transformation (FFT) and the Hamming window filter. An example is the spectral analysis of horizontal wind (u), vertical velocity (w), temperature (T), and specific humidity (q) at 1500 LST 20 May 1998, with the usual dimensionless frequency $f(nz/L)$ on the abscissa and the scheme-normalization parameters of Kaimal et al. (1972) on the ordinate (Fig. 1). The various elements have a maximum at low frequencies and a clear inertial domain at high frequencies. The energy dissipates with a power law and a slope of $-2/3$ (solid line), which indicates that the system is generally isotropic. The maximum longitudinal spectral frequency f_m reaches ~ 0.005, and the maximum frequency f_m of the vertical velocity spectrum ranges between 0.05 and 0.08, which is close to the $f_{mw} \approx 5f_{mu} = 2f_{mv}$ from the HEIFE Experiment (Wang et al., 1993). If the f_m of the vertical spectrum is assumed to be 0.065, the maximum dominant vortex would have a vertical scale of $L_m = 2/f_m \approx 30$ m. The f_m of the temperature spectrum is on the order of 0.06, slightly smaller than the one for specific humidity (0.08). Of the various spectra, f_m is lowest for the horizontal wind. Specific humidity and temperature have the weakest and strongest energy spectra, respectively, which suggests the occurrence of turbulence during the dry periods. The slight upward bend at the inertial end of the spectrum for specific humidity may be an instrumental artifact.

Most of the spectra during unstable stratification in daylight follow a power law with a slope of $-2/3$, whereas many of the nighttime spectra for temperature and specific humidity do not, probably because stable stratification suppresses turbulence motion.

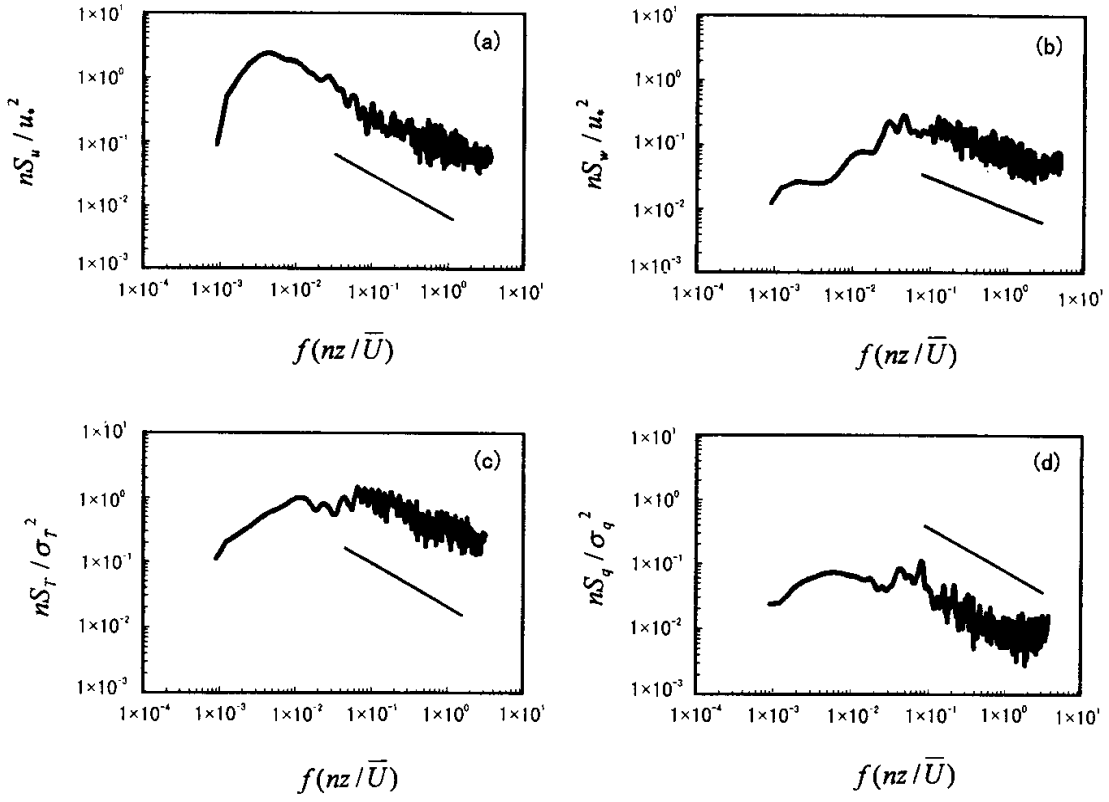

Fig. 1. Turbulence spectra of wind u (a), w (b), temperature (c), and specific humidity (d) at the Qamdo site.

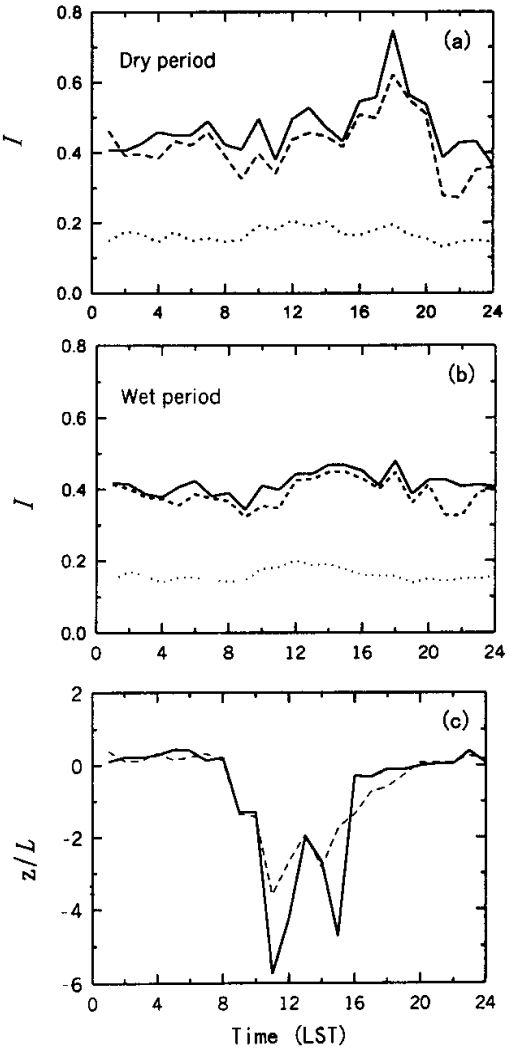

Fig. 2. Mean daily course of turbulence intensity (I) and stability (z/L) in the dry (a) and wet (b) period where the solid line denotes I_u, dashed I_v, and dotted I_w. z/L(c) is represented by a solid (dashed) line for the dry (wet) period.

3. Turbulence intensity

Because the Qamdo area often experienced thunderstorm after 23 May, generally from early evening into the night, we defined that date as the beginning of the wet period. The difference in air temperature between 0.5 m and 8 m is obviously greater in the dry period than in the wet period, while the difference in specific humidity is just the reverse, i.e., there is a distinct contrast in the two periods.

The averaged daily variation of turbulence intensity (I) showed that the intensity was much larger in the dry period than in the wet period with $I_u > I_v > I_w$ (Fig. 2). The stratification approached the unstable state ($z/L < 0$) from 0800 LST while the turbulence began to intensify. After 1500 LST, the turbulence developed vigorously and reached a maximum around 1800 LST, after which the turbulence was suppressed and the intensity reduced by the return to neutrality or stability ($z/L > 0$) in the dry period. The turbulence was enhanced in a rather smooth way with no significant peak displayed, except that its intensity was larger during the daytime in the wet period. For this reason, the thermal effect was dominant in the strengthening of turbulence at the Qamdo site.

4. Turbulent variance analysis

The variances of the 3D winds, temperature, and specific humidity in the near-surface layer were then normalized by frictional velocity (u_*), scale temperature (T_*), and scale humidity (q_*), respectively. By similarity theory, these should be functions of stability, and were expressed as

$$\sigma_a/u_* = \phi_a(z/L)\,, \qquad a = u, v, w \tag{1}$$

$$\sigma_T/|T_*| = \phi_t(z/L)\,, \tag{2}$$

$$\sigma_q/|q_*| = \phi_q(z/L)\,, \tag{3}$$

where $T_* = -\overline{w'T'}/u_*, q_* = -\overline{w'q'}/u_*$, and ϕ_a, ϕ_t, and ϕ_q stand for the universal functions of the variance of 3D winds, temperature, and specific humidity, respectively. The normalized variance of 3D winds for the neutral stratification in the near-surface layer is known to be approximately constant, i.e., $\sigma_u = Au_*$, $\sigma_v = Bu_*$ and $\sigma_w = Cu_*$.

Panofsky and Dutton (1984) reported values for A, B and C over different surfaces of a plain. The relation between variance of the horizontal winds and z/L in unstable stratification generally follow a 1/3-power law, i.e., $\sigma_{uv}/u_* = (-z/L)^{1/3}$, but this is controversial.

In order to ensure the high quality of the variance analysis of all variables and to eliminate the effects of local landform, the data during and after rain events, wind speeds less than 1 m s^{-1}, and unrealistic wind directions were removed. Figure 3 depicts the relations between the normalized variances of the 3D winds and z/L at the Qamdo and Gerze sites, indicating that the relationship satisfies the 1/3-power law in the unstable cases ($z/L < 0$) but tends to approach constants in

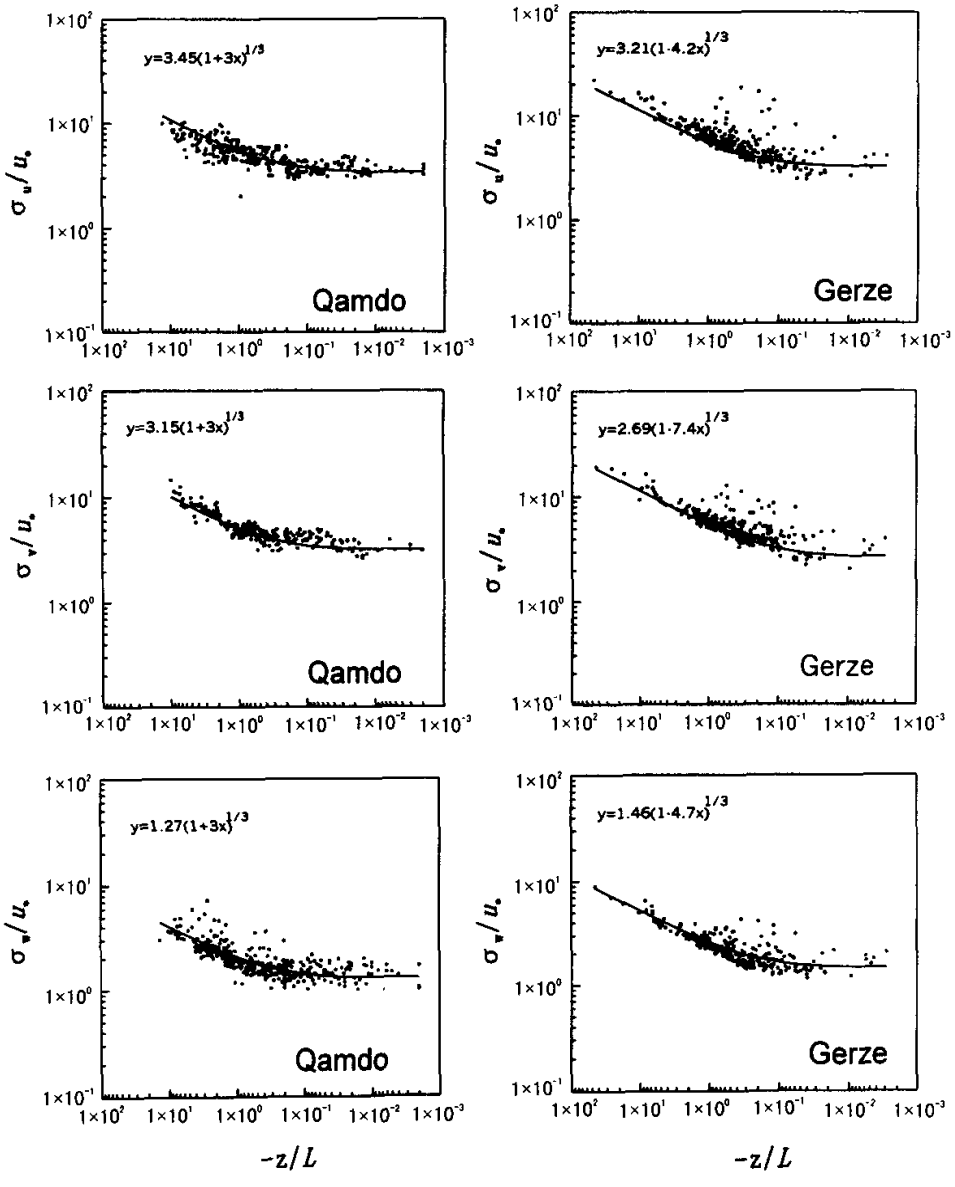

Fig. 3. Relation between normalized variances of 3D winds and $-z/L$ at the Qamdo and Gerze sites.

the near-neutral cases. This leads to the following fitted curves:

$$\sigma_u/u_* = 3.45(1-3z/L)^{1/3}, \quad z/L<0, \quad (4)$$

$$\sigma_v/u_* = 3.15(1-3z/L)^{1/3}, \quad z/L<0, \quad (5)$$

$$\sigma_w/u_* = 1.3(1-30z/L)^{1/3}, \quad z/L<0, \quad (6)$$

In their study of marine data, Hedde and Darand (1994) showed that σ_u/u_* and and σ_v/u_* are not related to z/L by a 1/3-power law, but rather that $\sigma_u/u_* = 2.0$ and $\sigma_v/u_* = 1.3$ for near-neutral stability. On the other hand, Panofsky and Dutton (1984) showed that σ_u/u_* and σ_v/u_* were related to z/L by a 1/3-power law. Thus the relations between variables depend on the sites under investigation.

Wyngaard and Cote (1974) suggested that the normalized variance of vertical velocity was related to z/L as follows:

$$\sigma_w/u_* = [1.6 - 2.9(z/L)^{2/3}]^{1/2} . \quad (7)$$

Panofsky and Dutton (1984) formulated the following empirical similarity function for unstable stratification over a homogeneous surface:

$$\sigma_w/u_* = 1.25(1 - 3z/L)^{1/3} . \quad (8)$$

Thus the relationship pattern between σ_w/u_* and z/L at both sites (Fig. 3) is very similar and close to that of Panofsky and Dutton (1984) except the constant of (6) differs locally from that of (8). Although Qamdo and Gerze are located in the regions of the Plateau that are different from plain regions, it is not only the relations between σ_w/u_* and z/L but also the variances of the horizontal winds that demonstrate they meet the similarity law.

The expressions (4)–(6) for the fitted curves of dimensionless wind variance versus z/L further reveals that with $z/L \approx 0$ for neutral stratification, $\sigma_u/u_*, \sigma_v/u_*$, and σ_w/u_* are close to constants, A, B and C, respectively. Table 1 shows the values these constants over rugged terrain in a near-neutral stratification case from TIPEX and other sources (Qi and Wang, 1996; Panofsky et al., 1977). One can see that $A > B > C$ occurs and the observed A and B are bigger in a rugged region than on a plain. The values of A and B are comparable from TIPEX sites and rugged areas but lower than those from Rock Spring, PA. The value of C is quite close to that from an uneven terrain and Rock Spring PA, except for the Damxung site which is located in middle of the Plateau. This fact demonstrates that the landform around the observing site has less impact on vertical turbulence compared to its influence on horizontal turbulence motion.

The variances of nondimensional temperature and specific humidity in unstable stratification cases can be expressed as

$$\sigma_T/|T_*| = \beta(-z/L)^{-1/3} , \quad (9)$$

$$\sigma_q/|q_*| = \beta(-z/L)^{-1/3} , \quad (10)$$

where β is a constant. The relationships of $\sigma_T/|T_*|$ and $\sigma_q/|q_*|$ to z/L depend on stability. In unstable conditions, $\sigma_T/|T_*|$ and z/L are related by a 1/3-power law, whereas in stable conditions, $\sigma_T/|T_*|$ decreases with increasing z/L, both being almost unrelated to their universal functions (Fig. 4). Analogous results for Nagqu, Tibet were found from the variance analysis of data taken during the same period (Hirohiko et al., 1999). Using data at Qamdo (11) and Gerze (12) under unstable stratification, we found that $\sigma_T/|T_*|$ and z/L were related in the following way:

$$\sigma_T/|T_*| = 1.10(-z/L)^{-1/3} , \quad (11)$$

$$\sigma_T/|q_*| = 1.21(-z/L)^{-1/3} . \quad (12)$$

The normalized variance of temperature has been studied much less. From the concept of mixed length, Panofsky et al. (1984) found that σ_T/T_* and z/L during unstable stratification were related as follows:

$$\sigma_T/|T_*| = 5(1 - 16z/L)^{1/2} . \quad (13)$$

Measurements of turbulence during the Heihe Field Experiment (HEIHE) allowed Wang et al. (1993) to derive

$$\sigma_T/|T_*| = 0.96(z/L)^{-1/3} , \quad z/L \le -0.35 . \quad (14)$$

Thus the relations between $\sigma_T/|T_*|$ and z/L at Qamdo and Gerze that we derived Eqs.(11) and (12) are similar to those of Wang et al. (1993), but differ greatly from those of Panofsky and Dutton (1984). Also, the divergence augmented in a near-neutral condition may be ascribed to weak convection and turbulence heat fluxes that are too small and too variable to be measured precisely.

Note that from Fig. 4 one can see that the variations of $\sigma_q/|q_*|$ with z/L diverge considerably more than $\sigma_T/|T_*|$ versus z/L. The best fit of $\sigma_q/|q_*|$ to z/L for unstable stratification at the Qamdo (15) and (16) Gerze sites are

$$\sigma_q/|q_*| = 1.60(z/L)^{-1/3} , \quad (15)$$

$$\sigma_q/|q_*| = 1.37(z/L)^{-1/3} . \quad (16)$$

Table 1. Dimensionless variances of 3D winds under near neutral stratification

Sites	$\sigma_u/u_* = A$	$\sigma_v/u_* = B$	$\sigma_w/u_* = C$	reference
Qamdo	3.45	3.15	1.30	TIPEX
Damxung	3.40	2.45	1.15	Zhou et al. (2000)
Gerze	3.21	2.69	1.46	TIPEX
Wudaoliang	2.98	2.91	1.35	Qi et al. (1996)
Erie, CO (rugged terrain)	2.65	2.00	1.20	Panofsky and Dutton (1984)
Rock Spring, PA (rugged terrain)	3.20	2.90	1.24	Same
Rock Spring, PA (mountain)	3.50	3.80	1.24	Same

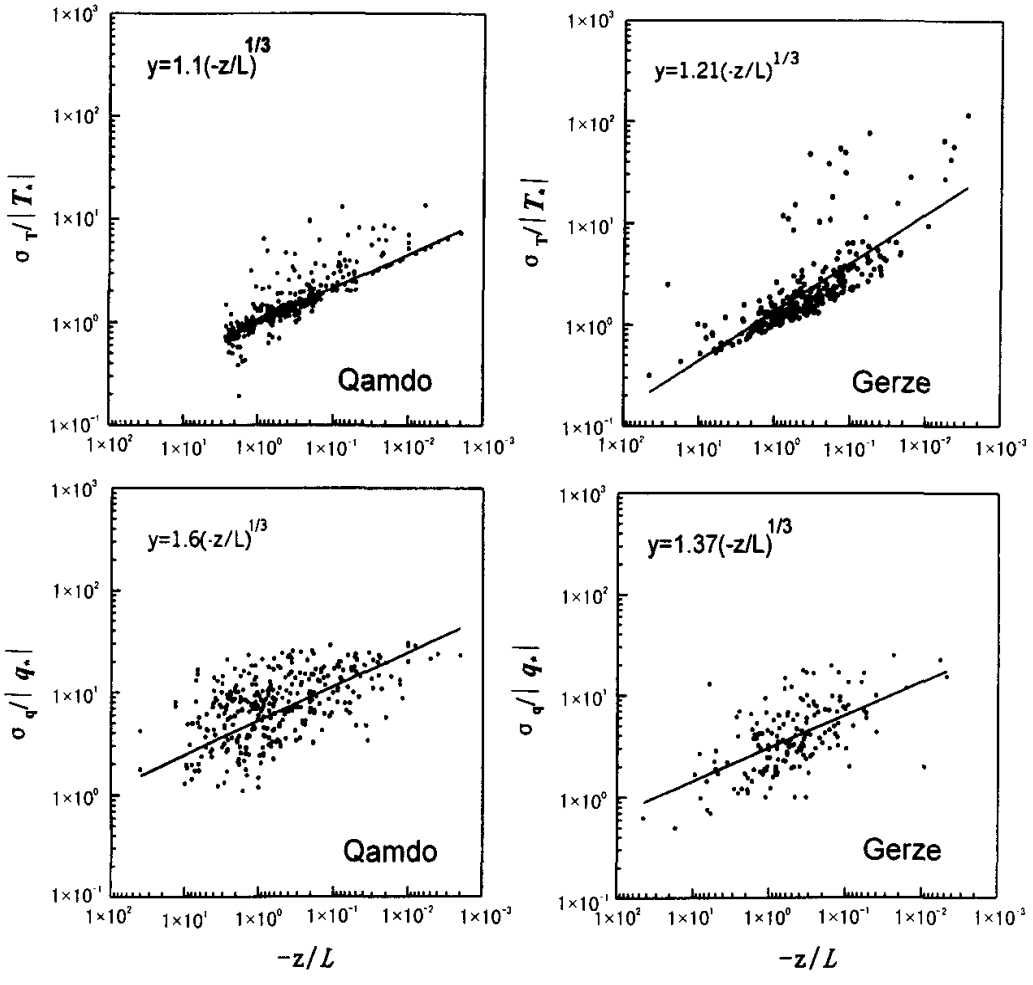

Fig. 4. Relations of $\sigma_T/|T_*|$ and $\sigma_q/|q_*|$ to z/L at the Qamdo and Gerze sites.

These curves, although nearly a 1/3 power law under unstable conditions, display conspicuous scatter. The relation of the similarity law does not hold under the stable condition as the divergence is too great between $\sigma_q/|q_*|$ and z/L.

In their study of data over a plain, Hogstrom and Semdman-Hogstrom (1974) indicated that $\sigma_q/|q_*|$ and z/L during the convective conditions follow the 1/3 power law with a constant $\beta=1.04$. It follows that the results (15) and (16) from the measurements made in the Plateau during an unstable case are compatible with the relation between $\sigma_q/|q_*|$ and z/L over plains except with larger values of β over the Plateau.

5. Features of heat source intensity

Since the Plateau surface heats the atmosphere by turbulence exchange and radiation processes, the heat balance equation for the underlying surface is expressed as

$$H + LE = R_n - Q_s\,, \tag{17}$$

where H is sensible heat and LE latent heat observed by eddy correlation, R_n net radiation measured, and Q_s soil heat flux obtained by soil flux plates and temperature gradients. The terms (H+LE) and (R_n-Q_s) of Eq.(17) are both referred to as the heating intensity. Here we use $H+LE$ to reveal how net radiation absorbed at the surface heats the atmosphere by

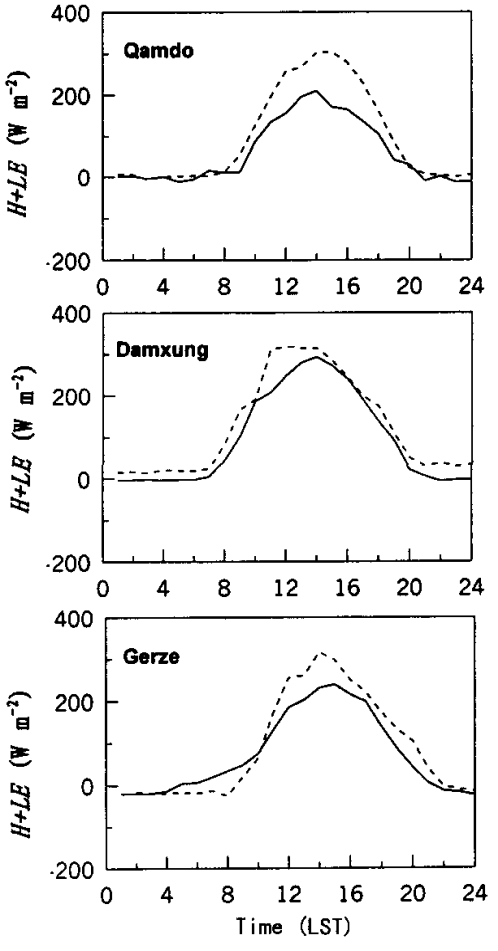

Fig. 5. Mean daily course of heat source intensity for the dry (solid line) and wet (dashed line) periods at the Qamdo, Damxung, and Gerze sites.

transferring heat via turbulence and evaporation.

Figure 5 presents the mean daily variation of heat source intensity ($H+LE$) for the dry and wet periods at the Qamdo, Damxung, and Gerze sites. It indicates that the pattern of the simple daily course at the three sites is quite similar and around midday, there is a noticeable maximum and in early morning a minimum in both periods, which are determined by the daily cycle of solar radiation. Remarkably, $H+LE$ during the wet period is larger than in the dry period. The biggest daily peak of $H+LE$ associated with the Damxung site reached 260 and 323 W m^{-2} for the dry and wet periods, respectively. The peaks are 239 and 317 W m^{-2} for the Gerze site, and 210 and 305 W m^{-2} for the Qamdo site for the respective periods. On average, from 0900 to 1900 LST, the surface transfers heat by turbulence motion, and during the night the surface absorbs heat from the air with small turbulence flux.

Table 2 summarizes the turbulence heat flux and heating intensity measured simultaneously at the TIPEX sites. It indicates that the sensible (latent) heat fluxes constitute 81% (19%) for Gerze, 96% (4%) for Damxung, and 82% (18%) for Qamdo of the heating intensity in the dry period. Thereafter, the latent (sensible) heat transport makes up 48% (52%) for Gerze, 47% (53%) for Damxung, and 64% (36%) for Qamdo of the heating intensity in the wet period. We can therefore say that the sensible heat is the main constituent of the heating flux during the dry period, and that the latent heat increases to become a higher proportion of the total heating during the wet period. Further, the total heating is also greatly increased at the three sites, in which it reaches >100 W m^{-2} at Damxung, during the wet period.

Table 2 also shows that after the monsoon onset, the observed cloudiness and precipitation simultaneously increase significantly, and are accompanied by storm weather. It follows that the intensification of the surface heating is responsible for augmented quantities of vapor transported in the form of latent heat into the air from the ground. This increases the potential energy available to produce eddy disturbance over the Plateau, triggering the growth of cloudy weather and rainfall, which is a feedback between the surface heating and the weather pattern. Zhu and Zhao (1987) reported their study on the feedback.

In order to better understand the difference of heating source intensities on the Plateau, we examine the average summer heat fluxes and surface energy budget components obtained from TIPEX and QXPMEX, as shown in Table 3. This demonstrates that although there was a difference in observation techniques, facilities, and methods between TIPEX and QXPMEX, the heat fluxes and energy components are to some extent comparable and representatives of the different sites on the Plateau.

It is necessary to indicate that the turbulence flux of TIPEX measured by eddy correlation came with a certain error of energy balance closure, while the turbulence flux of QXPMEX obtained by the profile and thermal equilibrium methods came without closure error. However the closure error (10%) between $H+LE$ and $R_n - Q_s$ at the Gerze site was smaller than the other two sites, 16% and 38% for Qamdo and Damxung, respectively. The error is high at Damxung, but the closure errors at Gerze and Qamdo are acceptable compared with many reports (Gu et al., 1999; Li et al., 1999). There are several possible reasons for the

Table 2. Turbulent heat fluxes (W m^{-2}) during the TIPEX

Site	Period	H	LE	$H+LE$
Gerze	Dry	46.0	11.0	57.0
	Wet	44.0	41.0	85.0
Damxung	Dry	74.2	2.8	77.0
	Wet	57.5	50.0	107.5
Qamdo	Dry	53.7	11.5	65.2
	Wet	33.8	60.6	94.4

Table 3. Comparison of summer heat components from different sites in the Tibetan Plateau

Sites	Above msl (m)	Latitude (N)	Longitude (E)	H (W m^{-2})	LE (W m^{-2})	Q_s (W m^{-2})	R_n (W m^{-2})	Source
Qamdo	3227	31°96′	97°16′	41.2	34.2	10.2	106.1	TIPEX
Lhasa	3633	29°42′	91°08′	73.5	42.9	11.0	133.9	Chen and Wen (1984)
Damxung	4260	30°02′	91°06′	65.9	26.4	7.7	157.4	TIPEX
Nagqu	4507	31°29′	92°03′	71.7	24.1	11.0	112.3	Chen and Wen (1984)
Shuanghu	4290	32°38′	89°00′	75.6	39.0	9.8	124.4	Chen and Wen (1984)
Shiquanhe	4278	32°30′	80°05′	68.8	31.2	9.7	109.7	Chen et al., ((1984)
Gerze	4200	32°13′	84°48′	45.0	26.0	14.0	92.5	TIPEX

closure are errors. The vapor turbulence measurements are less accurate compared to their temperature counterparts, erratic fluctuations may be affected by the surrounding complicated topography, and dew occurring on the surface of various sensors in the clear sky night could produce accumulative errors in the data.

The evidence indicate that $H+LE$ or R_n-Q_s at Qamdo, southeast Tibet and Gerze and Shiquanhe, western Tibet is lower than over the middle of the Tibetan Plateau from 91°E to 89°E during the summer. The sensible heat is a considerable proportion of the heating intensity, and the latent heat exhibits no significant difference between the eastern and western parts of the Plateau. It is noticeable that the largest heating intensity is over the central Plateau with $(H+LE)$ or $(R_n–Q_s) > 100$ W m^{-2} which should be considered in the boundary-layer parameterization schemes for the Plateau in numerical models.

6. Momentum flux

The daily mean course of momentum flux (τ) and wind speed (U) are shown in Fig. 6, which indicates that they display noticeable daily cycles but that these are in opposite phases in the two periods. The momentum transfer is enhanced with the increasing wind during the afternoon. The daily peak appears at 1800 LST and the sub-peak at 2000 LST during the dry period. The transfer is reduced to a great extent due to the effect of overcast and cloudy conditions in the wet period. The fluxes are exceedingly small from 0000 to 1000 LST in both periods. The pattern of the daily course at Qamdo is roughly analogous to that at Gerze, based on synchronous measurements (Li et al., 1999), but the flux intensity is higher than at Gerze.

7. Conclusions

By applying the eddy correlation method to data from TIPEX, the characteristics of turbulence transfer parameters for Qamdo in the southeastern Plateau are presented and compared with the results obtained in the middle and western Tibetan Plateau. This study provides a first understanding of the turbulence structure and transport characteristics for the summertime near-surface layer of that part of the Plateau.

Most of the spectra of the 3D winds, temperature, and humidity during the convection cases follow a power law with a slope of 2/3. The normalized variances of the 3D winds in relation to z/L stable and unstable stratification satisfy the similarity law but the normalized variances of temperature and humidity are related to the stratification by a $-1/3$ power law only in unstable conditions. Under stable stratification, their relation to z/L is scattered. In near-neutral stratification, σ_u/u_* and σ_v/u_* are similar to those in a rugged terrain and σ_w/u_* is similar to that in plains. The evidence indicates that effects of landform on the vertical turbulence are not significant and differ from the effects of horizontal winds over the southeast and western Tibetan Plateau.

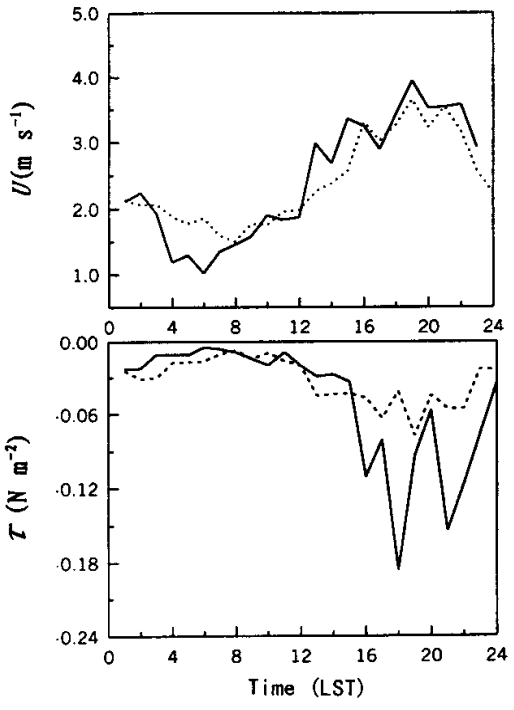

Fig. 6. Daily mean course of momentum flux (τ) and wind speed (U).

At the Qamdo site during the dry period, the sensible heat dominates, comprising 81% of the heat intensity with the other 19% being latent heat; in the wet period on the other hand, the latent heat is larger at 64% of the heating intensity while the sensible heat fraction is less at 36%. On average, the intensity of the heating of air in the southeastern and western Plateau is lower than in the middle Plateau during the summer. The maximum heating intensity occurs in the central area of the Tibetan Plateau.

Acknowledgments. The authors are grateful to the Tibetan Qamdo Regional Weather Bureau for their assistance in the field work, to the Japanese side of the Sinn-Japan GAME/Tibet Cooperation for their facilities, to the chief scientists, Prof. Tao Shin and Prof. Chen Lianshou, and the team members, to Prof. Chen Jiayi and in particular, to Academician Zhou Xiuji for his suggestions and comments on the manuscript. This work was supported by National Key Program (85-1-38) and National Science foundation of China

REFERENCES

Bian Lingen, Lu Longhua, Cheng Yanjie, and Lu Changgui, 2001: Turbulent measurement over the southeastern Tibetan Plateau. *Quart. Journal of Applied Meteorology*, **12**(1), 1–12. (in Chinese)

Chen Wanlong, and Wen Duming, 1984: The computing method research of observations ten-days total sensible and latent heat on Tibetan Plateau. Proceedings of QXPMEX (II), Beijing: Science Press, 38–39. (in Chinese)

Gu, J., E. A. Smith, and J. D. Merritt, 1999: Testing energy balance closure with GOES-retrieved net radiation and in situ measured eddy correlation fluxes in BOREAS. *Journal of Geophysical Research*, **104**(22), 27881–27893.

Hedde, T., and P. Darand, 1994: Turbulence intensities and bulk coefficients in the surface layer above sea. *Boundary-Layer Meteorology*, **71**, 415–432.

Hirohiko, I., H. Taichi, and T. Kenji, 1999: Summary of planetary boundary layer observation in GAME/TIBET. Proceedings of the 1st International Workshop on GAME/Tibet, Xi'an, China, 11–13 Jan., 69–76.

Hogstrom, U., and A. S. Semdman-Hogstrom, 1974: Turbulence mechanics at an agricultural site. *Boundary-Layer Meteorology*, **7**, 373–389.

Kaimal, J. C., J. C. Wyngaard, and Y. Izumi, 1972: Spectral characteristics of surface layer turblence. *Quart J. Roy. Meteor. Soc.*, **98**, 563–589.

Li Jialun, Hong Zhongxiang, and Luo Weidong., 1999: Turbulent observations of near surface in Gaize of Tibetan Plateau. *Chinese J. Atmos. Sci.*, **2**(23), 142–151. (in Chinese)

Panofsky, H. A., H. Tenekes, and D. H. Lenschow, 1977: The characteristics of turbulence volocity components in the surface layer under convective conditions. *Boundary-Layer Meteorology*, **11**, 355–361.

Panofsky, H. A., D. Larko, and R. Lipschutz, 1982: Spectra of velocity components and complex terrain. *Quart J. Roy. Meteor. Soc.*, **108**, 215–230.

Panofsky, H. A., and J. A. Dutton, 1984: *Atmospheric Turbulence*. New York: John Willy and Sons, 10–50.

Qi Yongqiang, and Wang Jiemin, 1996: The Characteristics of turbulence transfer in wudaoliang area in Tibetan Plateau. *Plateau Meteorology*, **15**(2), 172–177. (in Chinese)

Wang Jiemin, Liu Xiaohu, and Ma Yaoming, 1993: The turbulence transfer characteristics and its structure at low surface of boundary layer in Gobi area during HEIFE experiment. *Acta Meteorological Sinica*, **3**(51), 343–349. (in Chinese)

Wyngaard, J. C., and O. R. Cote, 1974: Volution of a convective planetary boundary layer A high-order-closure model study. *Boundary-Layer Meteorology*, **7**, 289–308.

Zhang Jijia, Zhu Baozhen, and Zhu Fukang, 1988: *The Advance of Tibetan Plateau Meteorology*, Beijing: Science Press,. 1–265. (in Chinese)

Zhou Mingyu, Xu Xiangde, and Bian Lingen, 2000: *Observational Analysis and Dynamic Study of Atmospheric Boundary Layer on Tibetan Plateau.*, Beijing: China Meteorological Press, 3–20, 120pp. (in Chinese)

Zhou Xiuji, Tao Shanchang, and Yao Keya, 1991: *Atmospheric Physics*, Beijing: China Meteorological Press, 206–236. (in Chinese)

Zhu Fukang, and Zhao Wei, 1987: Some observation results of surface net radiation and its impact on the general circulation on Tibetan Plateau. *Proceeding of QXPMEX (III)*, Beijing: Science Press, 54–61. (in Chinese)

TIPEX高原东南部近地层湍流参数的分析

卞林根 徐祥德 陆龙骅 高志球 周明煜 刘辉志

摘 要

利用第二次青藏高原科学试验(TIPEX)涡旋相关法资料，计算和分析了高原东南部湍流谱、三维风速、温度和湿度归一化的方差和近地面湍流通量。结果表明，白天在不稳定层结条件下，大部分湍流谱基本能满足-2/3次方定律。三维风速、温度和湿度归一化的方差与稳定度的关系在不稳定条件下基本服从1/3次方定律，温度和湿度方差在稳定层结下与稳定度1/3次方定律的关系不显著。昌都和改则中性层结下的A、B值比平原地区大，与起伏地形的值接近，高原东南部和西部的C 值没有显著差异，与在平原地区的差异不大,表明观测区的地形对垂直方向的湍流没有明显影响。昌都干期的热源强度以感热为主（81%），潜热约占19%，湿期的热源强度有所增大；潜热占64%，感热占36%。与高原其它站的观测结果相比表明，夏季最大加热强度出现在高原中部。

关键词：青藏高原, 涡旋相关, 方差分析, 热源